

Figure 6. Proposed mechanism for Reppe hydroformylation.

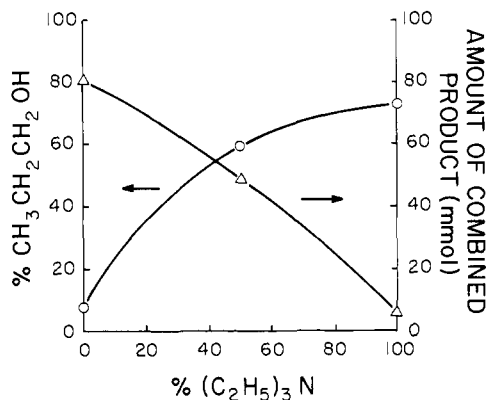
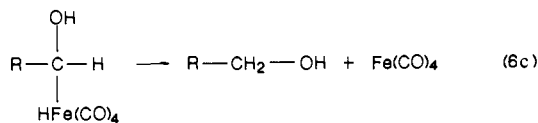
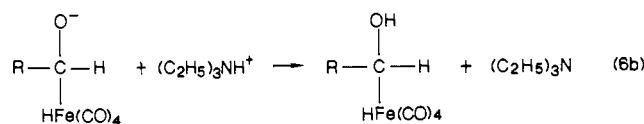
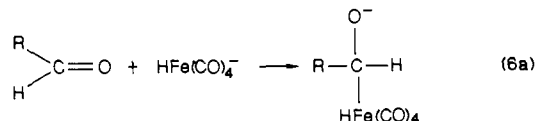


Figure 7. Percentage of product in the form of 1-propanol (O) and overall production after 6 h (Δ) shown as a function of base composition. Catalyst solution: Fe(CO)<sub>5</sub> (4.4 mmol), total base (36 mmol), 200 mL (25% H<sub>2</sub>O, 75% CH<sub>3</sub>OH v/v). Temperature: 110 °C. Loading pressures at 25 °C: P(CO) = 300 psig, P(C<sub>2</sub>H<sub>4</sub>) = 160 psig.

49 mmol of combined product was formed over 6 h. However, the yield of alcohol was greatly enhanced with 1-propanol now constituting 60% of the combined product. The reaction proceeded still more slowly when 100% triethylamine (36 mmol of (C<sub>2</sub>H<sub>5</sub>)<sub>3</sub>N) was employed. In this case only 6 mmol of product was formed after 6 h with the product mixture now consisting of 73% 1-

propanol and 27% propionaldehyde. These data, shown graphically in Figure 7, clearly illustrate the antithetic changes in alcohol yield and overall rate of reaction that accompany the substitution of triethylamine for sodium hydroxide.

Markó and co-workers<sup>8</sup> have shown that in aqueous solutions triethylammonium hydridotetracarbonylferrate [(C<sub>2</sub>H<sub>5</sub>)<sub>3</sub>NH]<sup>+</sup>[HFe(CO)<sub>4</sub>]<sup>-</sup> rapidly reduces 1-butyraldehyde to 1-butanol while the corresponding sodium salt (NaHFe(CO)<sub>4</sub>) was unreactive under the same mild conditions. They attribute the reactivity of the trialkylammonium salt to the ease with which the triethylammonium ion can protonate the aldehyde-hydrido-tetracarbonylferrate adduct in the second step (eq 6b) of the mechanism shown below (R = C<sub>3</sub>H<sub>7</sub>). When NaHFe(CO)<sub>4</sub> is



used, water or alcohol molecules of the solvent system must serve as proton donors. These are very weak acids compared to (C<sub>2</sub>H<sub>5</sub>)<sub>3</sub>NH<sup>+</sup>. As a result, the rate of protonation of the aldehyde-hydrido-tetracarbonylferrate adduct is quite slow. The results shown in Figure 7 are clearly in accord with the observations of Markó and co-workers. While the volatility of triethylamine may be a factor, the decrease in the rate of the hydroformylation reaction when (C<sub>2</sub>H<sub>5</sub>)<sub>3</sub>N is substituted for NaOH most likely reflects a decrease in the steady-state concentration of HFe(CO)<sub>4</sub><sup>-</sup> due to the slower rate of production of HFe(CO)<sub>4</sub><sup>-</sup> from the Fe(CO)<sub>5</sub> produced by step 5 of the catalytic cycle resulting from the weaker basicity of triethylamine.

**Acknowledgment.** The authors express appreciation for the support provided by the Division of Basic Sciences of the U.S. Department of Energy (Contract EY-76-S-09-0933).

## Cation- or Solvent-Induced Supramolecular Phthalocyanine Formation: Crown Ether Substituted Phthalocyanines

Nagao Kobayashi\*<sup>1</sup> and A. B. P. Lever\*

Contribution from the Department of Chemistry, York University, North York, Toronto, Ontario, Canada M3J 1P3. Received February 24, 1987

**Abstract:** Phthalocyanines with four 15-crown-5 ether voids at the 3,4-positions (MtCRPc) (Mt = H<sub>2</sub>, Zn, Co, Ni, Cu) have been synthesized and characterized. Dimerization of MtCRPc is induced in solvents such as methanol and by addition of some cations (K<sup>+</sup>, Ca<sup>2+</sup>, NH<sub>4</sub><sup>+</sup>), especially K<sup>+</sup>. Cofacial dimer formation in the presence of these cations proceeds in a two-step three-stage process, as indicated by absorption and emission spectroscopy. These species have a highly specific D<sub>4h</sub> eclipsed configuration providing well-defined dimeric species for spectroscopic analysis. The ESR spectrum of the cation-induced dimeric CuCRPc shows axial symmetry and may be analyzed in terms of an interplanar separation of 4.1 Å. The <sup>1</sup>H NMR spectra of the cation-induced metal-free and zinc dimers are consistent with an eclipsed configuration. Upper excited state (Soret, S<sub>2</sub>) emission is observed for the first time in the phthalocyanine series.

Dimerization, often through aggregation of porphyrins<sup>2</sup> and phthalocyanines,<sup>3</sup> has been intensively investigated. In general

the mechanics of aggregation is poorly understood, the product may be contaminated with monomer and perhaps with higher

**Table I.** Elemental Analytical Data of MtCRPcs<sup>a</sup>

compd	% C		% H		% N	
	found	calcd	found	calcd	found	calcd
H <sub>2</sub> CRPc	59.83	60.27	5.74	5.85	8.78	8.79
ZnCRPc	57.25	57.42	5.37	5.42	8.37	8.37
CuCRPc	57.33	57.50	5.36	5.43	8.29	8.38
NiCRPc	57.51	57.71	5.35	5.45	8.30	8.41
CoCRPc	57.54	57.70	5.38	5.45	8.29	8.41

<sup>a</sup>Theoretical values are calculated for C<sub>64</sub>H<sub>72</sub>N<sub>8</sub>O<sub>20</sub>Mt<sub>1</sub> except for H<sub>2</sub>CRPc(C<sub>64</sub>H<sub>72</sub>N<sub>8</sub>O<sub>20</sub>H<sub>2</sub>).

aggregates, and the relative orientation of the components is obscure. We report here the preparation of phthalocyanines functionalized at the 3,4-positions with four crown ether voids (MtCRPc),<sup>4</sup> together with their cation- or solvent-induced dimerization. Unambiguous evidence is presented which indicates the stepwise formation of two dimeric species induced by K<sup>+</sup> ions. The first is non-cofacial, while the second is a rigidly cofacial eclipsed *D*<sub>4h</sub> species. This provides the opportunity to study the UV/visible absorption and emission, ESR, and NMR spectra of well-defined dimeric species (metal free, Zn, Cu, Co, and Ni) in terms of exciton theory. Upper excited state S<sub>2</sub> emission is observed in phthalocyanine chemistry for the first time. The results are compared with corresponding data for the tetra-crowned porphyrins,<sup>6,7</sup> where the orientation is twisted. We refer to the dimerization of the monomeric MtCRPc units for ease of discussion while noting that the binuclear products contain one or more main group ions and are therefore not, strictly speaking, dimers of the mononuclear unit.

### Experimental Section

(i) **Measurements.** Electronic absorption spectra were recorded with a Perkin-Elmer Hitachi Model 340 microprocessor spectrometer. Emission and excitation spectra were obtained with a Varian SF330 spectrofluorimeter with appropriate filters to eliminate scattered light. Fluorescence quantum yields were determined by the use of quinine

(1) Visting Professor from the Pharmaceutical Institute, Tohoku University, Sendai, Japan.

(2) White, W. I. In *The Porphyrins*; Dolphin, D. Ed.; Academic Press: New York, 1978; Vol. V, p 303. Katz, J. J.; Shipman, L. L.; Cotton, T. M.; Janson, T. R. *Ibid.*, p 401. Kassel, D. *Photochem. Photobiol.* **1984**, *39*, 851. Basu, S.; Rohatgi-Mukherjee, K. K.; Arbeloa, I. L. *Spectrochem. Acta* **1986**, *42*, 1355. Shelnut, J. A.; Dobby, M. M.; Satterlee, J. D. *J. Phys. Chem.* **1984**, *88*, 4980.

(3) Sidorov, A. N.; Kotlyar, I. P. *Opt. Spectrosk.* **1961**, *11*, 92. Sheppard, S. E.; Geddes, S. E. *J. Am. Chem. Soc.* **1944**, *66*, 1995. Bernauer, K.; Fallab, S. *Helv. Chim. Acta* **1961**, *54*, 1287. Kratky, O.; Oelschaeger, H. *J. Colloid Interface Sci.* **1969**, *31*, 490. Shelly, Z. A.; Farina, R. D.; Eyring, E. M. *J. Phys. Chem.* **1970**, *74*, 617. Shelly, Z. A.; Harward, D. J.; Hemmes, P.; Eyring, E. M. *J. Phys. Chem.* **1970**, *74*, 3040. Siegl, H.; Waldmeier, P.; Puijs, B. *Inorg. Nucl. Chem. Lett.* **1971**, *7*, 161. Blagrove, R. J.; Gruen, L. C. *Aust. J. Chem.* **1972**, *25*, 1972. Monahan, A. R.; Brado, J. A.; DeLuka, A. F. *J. Phys. Chem.* **1972**, *76*, 446, 1994. Farina, F. D.; Halko, D. J.; Swinehart, J. H. *J. Phys. Chem.* **1972**, *76*, 2343. Boyd, P. D. W.; Smith, T. D. *J. Chem. Soc., Dalton Trans.* **1972**, 839. Abkowitz, M.; Monahan, A. R. *J. Chem. Phys.* **1973**, *58*, 2281. Gruen, L. C.; Blagrove, R. J. *Aust. J. Chem.* **1973**, *26*, 319. Abel, E. W.; Pratt, J. M.; Whelan, R. *J. Chem. Soc., Dalton Trans.* **1976**, 509. Cookson, D. J.; Smith, T. D.; Boas, J. F. *J. Chem. Soc., Dalton Trans.* **1976**, 1791. Harriman, A.; Richoux, M. C. *J. Chem. Soc., Faraday Trans. 2* **1980**, *73*, 1618. Darwent, J. R.; McCubbin, I.; Phillips, D. *J. Chem. Soc., Faraday Trans. 2* **1982**, *78*, 347, 903. Knoesel, R.; Piechocki, C.; Simon, J. *J. Photochem.* **1985**, *29*, 445.

(4) Abbreviations used in this study: Pc, phthalocyaninato dianion; CRPc, tetra(15-crown-5)ed phthalocyaninato dianion; ESR, electron spin resonance; FAB, fast atom bombardment; NMR, nuclear magnetic resonance; DPPH, diphenylpicrylhydrazyl; DCE, 1,2-dichloroethane; DMF, dimethylformamide; THF, tetrahydrofuran; FTIR, fourier transform infrared.

(5) Preliminary results on CuCRPc have been published: (a) Kobayashi, N.; Nishiyama, Y. *J. Chem. Soc., Chem. Commun.* **1986**, 1462. Two other reports on CuCRPc have appeared independently: (b) Koray, A. R.; Ahsen, V.; Bakaroglu, O. *J. Chem. Soc., Chem. Commun.* **1986**, 932; (c) Hendriks, R.; Sielcken, O. E.; Drenth, W.; Nolte, R. J. M. *Ibid.* **1986**, 1464.

(6) Kobayashi, N.; Osa, T. *Heterocycles* **1981**, *15*, 675.

(7) (a) Thanabal, V.; Krishnan, V. *J. Am. Chem. Soc.* **1982**, *102*, 3463. (b) Thanabal, V.; Krishnan, V. *Inorg. Chem.* **1982**, *21*, 3606. (c) Thanabal, V.; Krishnan, V. *Ibid.* **1985**, *24* 3253. (d) Chandrashekar, T. K.; Willigen, H.; Ebersole, M. H. *J. Phys. Chem.* **1985**, *89*, 3453. Willigen, H.; Chandrashekar, T. K. *J. Am. Chem. Soc.* **1986**, *108*, 709.

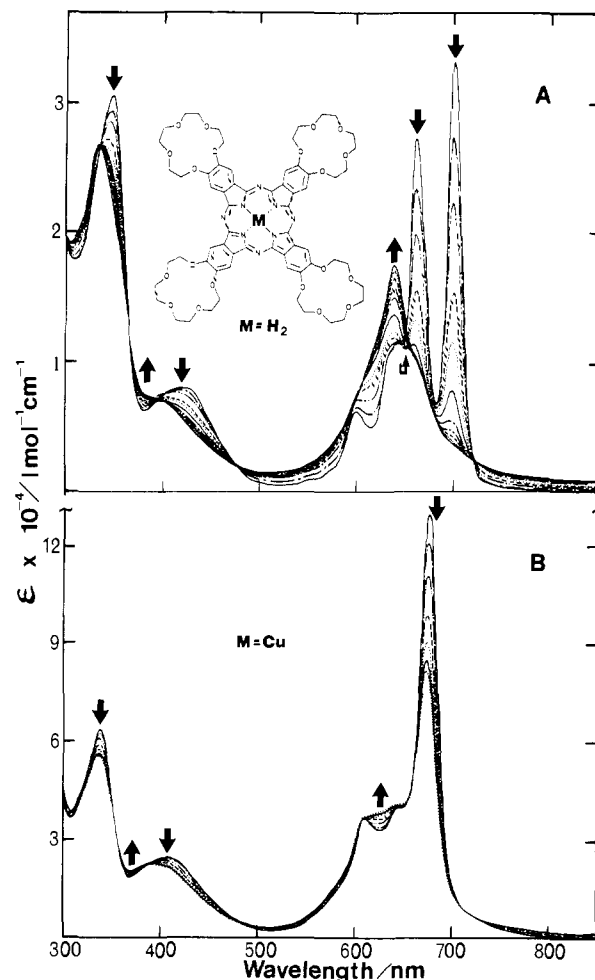


**Figure 1.** Change of absorption spectra of (A) H<sub>2</sub>CRPc and (B) CuCRPc (below) by the addition of CH<sub>3</sub>COOK or CH<sub>3</sub>COONa, respectively, to 3 mL of a CHCl<sub>3</sub> solution of H<sub>2</sub>CRPc or CuCRPc in a 10-mm cell. The CH<sub>3</sub>COOK and CH<sub>3</sub>COONa were each dissolved in CHCl<sub>3</sub>-MeOH (95:5 v/v) and were added with a microsyringe; 60 μL were added in all. Arrows indicate the direction of the spectroscopic change. In part B the final spectrum is that of a CH<sub>3</sub>COONa saturated solution.

bisulfate in 1 N H<sub>2</sub>SO<sub>4</sub> ( $\theta_F = 0.55$  at 296 K),<sup>8a,b</sup> or free base tetraphenylporphyrin in benzene ( $\theta_F = 0.11$ ).<sup>8c</sup> Data were obtained by a comparative calibration method with use of the same excitation wavelength and absorbance for the crown species and the calibrants and the same emission energies.

ESR measurements were obtained on a Varian E4 spectrometer, calibrated with DPPH. FTIR spectra were recorded on a Nicolet SX20 spectrometer, using KBr discs. <sup>1</sup>H NMR spectra were recorded on a Varian LH360 spectrometer with deuteriochloroform alone, or containing deuteriomethanol or tetramethylsilane as internal standard. The FAB mass spectra were obtained by courtesy of the Nebraska Center for Mass Spectroscopy by the same method as described previously.<sup>9</sup> Solvents, dimethylformamide, 1,2-dichloroethane, diethyl ether, methanol, ethanol, etc., were either distilled or Spectrograde.

(ii) **Synthesis.** 2,3-(3',4'-Dibromobenzo)-1,4,7,10,13-pentaoxacyclopentadeca-2-ene. Following the dibromination of 1,2-dimethoxybenzene,<sup>10</sup> so-called benzo-15-crown-5<sup>11</sup> was reacted with 2 equiv of bromine in acetic acid, using a small crystal of iodine as initiator. Recrystallization from ethanol gave colorless plates in 51% yield. Anal. Calcd for C<sub>14</sub>H<sub>18</sub>Br<sub>2</sub>O<sub>5</sub>: C, 39.5; H, 4.3. Found: C, 39.6; H, 4.3. <sup>1</sup>H NMR (CDCl<sub>3</sub>, internal Me<sub>4</sub>Si)  $\delta$  7.06 (2 H, s), 4.25–3.70 (16 H, m). mp. 80–81 °C.

(8) (a) Melhuish, W. H. *J. Phys. Chem.* **1960**, *64*, 762. (b) Demas, J. N.; Crosby, G. A. *Ibid.* **1971**, *75*, 991. (c) Seybold, P. G.; Gouterman, M. *J. Mol. Struct.* **1969**, *31*, 1.

(9) Leznoff, C. C.; Marcuccio, S. M.; Greenberg, S.; Lever, A. B. P.; Tomer, K. B. *Can. J. Chem.* **1985**, *63*, 623.

(10) Metz, J.; Schneider, O.; Hanack, M. *Inorg. Chem.* **1984**, *23*, 1065.

(11) Pedersen, C. J. *J. Am. Chem. Soc.* **1967**, *89*, 7017.

**Table II.** Characteristic Absorption Bands of MtCRPcs,<sup>a</sup> nm ( $\epsilon$ )

compd	monomeric species	$f^{b,c}$	half-bandwidth, $\text{cm}^{-1}$	dimeric cofacial species	$f$	half-bandwidth, $\text{cm}^{-1}$
H <sub>2</sub> CRPc	700 (33400)			639 (17500)		
	662 (27500)					
	645 (11800)					
	601 (6200)					
	421 (8100)			402 (sh) <sup>d</sup>		
ZnCRPc	347 (30800)	0.16	350	333 (26400)	0.17	730
	677 (96700)			635 (51000)		
	610 (17300)			580 (sh)		
	420 (sh)					
	352 (61200)			342 (53800)		
CuCRPc	676 (129400)	0.29	480	635 (74000)	0.35	1050
	610 (31200)			389 (21400)		
	409 (23300)			328 (51400)		
	338 (57400)					
	292 (54100)					
NiCRPc	667 (70000)	0.17	520	630 (47000)	0.18	845
	638 (22300)					
	603 (17700)					
	401 (14900)					
				385 (13700)		
CoCRPc	668 (59400)	0.20	750	627 (41200)	0.26	1400
	608 (19800)			571 (sh)		
	400 (13400)			390 (sh)		
	329 (sh)					
	297 (49300)			300 (45900)		

<sup>a</sup> Monomer spectra were collected in CHCl<sub>3</sub>, while those of dimer were in CHCl<sub>3</sub> containing ca. 0.1% MeOH and in the presence of K<sup>+</sup>(CH<sub>3</sub>COOK), [K<sup>+</sup>]/[MtCRPc] = 4. Extinction coefficient ( $\epsilon$ ) is per phthalocyanine unit. <sup>b</sup> Oscillator strength. <sup>c</sup> Oscillator strengths for the monomeric species are lower limits excluding higher energy vibrational satellites. <sup>d</sup> sh means shoulder.

**2,3-(3',4'-Dicyanobenzo)-1,4,7,10,13-pentaoxacyclopentadeca-2-ene.** The above dibrominated benzo-15-crown-5 (8.52 g, 0.02 mol) and CuCN (5.4 g, 0.06 mol) were refluxed in dry DMF (80 mL) for 5 h. After rotary evaporation of about 50–60 mL of DMF, concentrated ammonia (200 mL, 28%) was added, and air was bubbled through the solution for 12 h. After the solution was washed copiously with water, the dry olive-green product was Soxhlet extracted with diethyl ether for 3 days. Benzene recrystallization provided 2.02 g (31%) of colorless small needles. Anal. Calcd for C<sub>16</sub>H<sub>18</sub>N<sub>2</sub>O<sub>5</sub>: C, 60.4; H, 5.7; N, 8.8. Found: C, 60.1; H, 5.8; N, 8.5. <sup>1</sup>H NMR (CDCl<sub>3</sub>)  $\delta$  7.14 (2 H, s), 4.35–3.70 (16 H, m); IR (KBr)  $\nu$  2223 (C $\equiv$ N) cm<sup>-1</sup>; mp 151–2 °C.

**Nonmetalated (H<sub>2</sub>CRPc) and Metalated (MtCRPc) Crowned Phthalocyanines.** H<sub>2</sub>CRPc was prepared by refluxing benzo-15-crown-5 dicyanide (1.24 g, 3.9  $\times$  10<sup>-3</sup> mol) in 2-(dimethylamino)ethanol (5 mL) for 17 h while passing ammonia gas through the solution. The precipitate was re-precipitated from diethyl ether, washed with water, dried, and then chromatographed on basic alumina, initially with chloroform as eluant. The initial yellow band, which was discarded, was followed by a blue band which was eluted with ethanol–chloroform, providing 0.468 g (38%) of slightly bluish green powder (for analysis, see Table I). <sup>1</sup>H NMR (CDCl<sub>3</sub>)  $\delta$  8.02 (8 H, m), 4.7–3.6 (64 H, m), -3.41 (2 H, s).

ZnCRPc was obtained by reaction of H<sub>2</sub>CRPc with a large excess of zinc acetate in refluxing DCE/ethanol for several days in the dark, until the 4-band Q spectrum of H<sub>2</sub>CRPc had disappeared. After removal of the solvent, the residue was washed with water and recrystallized from chloroform–ethanol (78% yield). The FAB mass spectrum showed peaks at  $m/e$  values of 1339 (M<sup>+</sup>, 7), 956 (68), 522 (22), 460 (58), 424 (23), 307 (46), and 154 (100) (relative intensities in parentheses).

Other MtCRPcs (Mt = Co<sup>II</sup>, Fe<sup>II</sup>, Ni<sup>II</sup>, Cu<sup>II</sup>) were prepared by the "nitrile" method.<sup>12</sup> The benzo-15-crown-5 dinitrile and the appropriate metal acetate were refluxed gently in ethylene glycol<sup>10</sup> for several hours. The solution was filtered while hot, and the residue was washed with hot ethanol, hot water, and hot ethanol and then chromatographed on basic alumina, resulting in yields between 26 and 51% of the metalated products. Elemental analyses are presented in Table I.

## Results and Discussion

**(i) Cation Complexation Leading to Stepwise Cofacial Dimer Formation.** In chloroform solution, the several MtCRPc species exhibit spectra typical of well-behaved mononuclear metallo-phthalocyanines<sup>12</sup> generally with a single intense  $\pi$ - $\pi^*$  transition in the range 667–708 nm with associated higher energy vibrational components, commonly referred to as the Q band, and a second

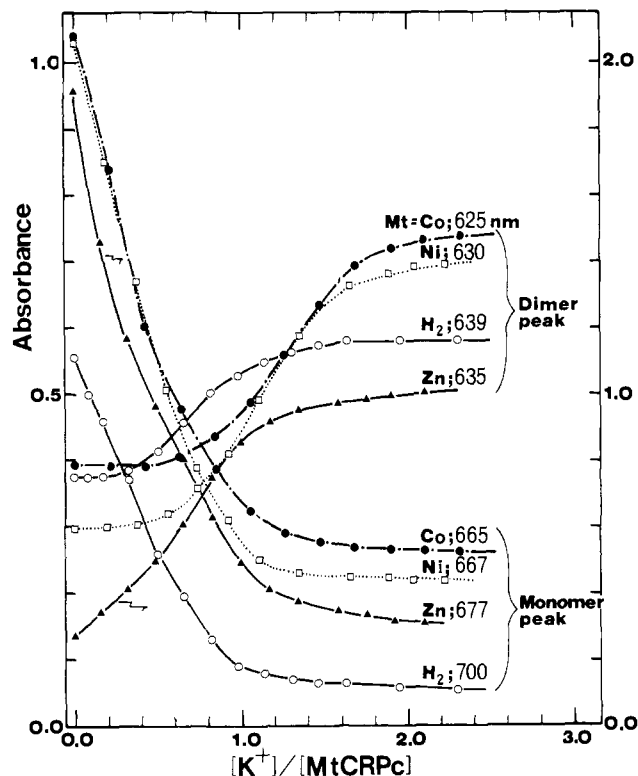


**Figure 2.** The dependence of absorbance of several MtCRPcs on [K<sup>+</sup>]/[MtCRPc] for several wavelengths. Experiments were conducted as described in Figure 1.

intense and broader  $\pi$ - $\pi^*$  transition at 300–360 nm called the Soret<sup>12</sup> (Table II; Figure 1). The metal-free species H<sub>2</sub>CRPc is similar but shows two closely spaced Q bands because of its lower (*D*<sub>2h</sub>) symmetry. As will be demonstrated below, dimerization occurs in many other solvents or when certain cations are added to this solution. Such dimerization is readily monitored by the dramatic change in absorption, and in particular by a blue shift in both the Soret and Q band absorption.<sup>13</sup>

In the case of porphyrins functionalized at the methine positions with four benzo-15-crown-5<sup>7a</sup> units, increasing addition of K<sup>+</sup>, NH<sub>4</sub><sup>+</sup>, and Ba<sup>2+</sup> ions affected the porphyrin Q band absorption by (a) a reduction in intensity, (b) broadening, and (c) a red shift of ca. 10 nm. On the other hand, Na<sup>+</sup>, Mg<sup>2+</sup>, and Ca<sup>2+</sup> did not cause any appreciable change in the visible region absorption. Note that the potassium ion is sandwiched between two crown ether units, and does not reside within the ether ring.

The MtCRPc species behave quite differently. Thus K<sup>+</sup>, NH<sub>4</sub><sup>+</sup>, Ca<sup>2+</sup>, and Na<sup>+</sup> all alter the spectra appreciably, though not all in the same fashion, while Ba<sup>2+</sup>, Cs<sup>+</sup>, and Mg<sup>2+</sup> have little effect. The ionic radii of cations which produce significant changes in the electronic spectra of the MtCRPc species are equal or smaller than those required in the porphyrin series.<sup>14</sup> In the crown phthalocyanine case, addition of K<sup>+</sup>, NH<sub>4</sub><sup>+</sup>, and Ca<sup>2+</sup> causes (a) a reduction in Q band intensity around 660–700 nm (the so-called monomer peak) and an increase in peak intensity around 620–640 nm (the so-called dimer peak), i.e., a blue shift of the Q band of ca. 30–60 nm, (b) a blue shift in the Soret (10–20 nm), and (c) some broadening in the Q band region (Figure 1A; Table II). Such changes are most obvious for K<sup>+</sup> with respect to the amount needed to affect them.

Absorbance intensities in the 660–700 and 620–640 nm ranges change markedly with K<sup>+</sup> concentration up to [K<sup>+</sup>]/[MtCRPc] = ca. 2. Previous experience with aggregated<sup>3</sup> and binuclear

(13) Dodsworth, E. S.; Lever, A. B. P.; Seymour, P.; Leznoff, C. C. *J. Phys. Chem.* **1985**, *89*, 5698.

(14) The cavity size of 15-crown-5 is estimated from CPK models to be 1.7–2.2 Å. The ionic diameters of the cations used in this paper are Mg<sup>2+</sup> 1.60 Å, Na<sup>+</sup> 1.90 Å, Ca<sup>2+</sup> 1.98 Å, K<sup>+</sup> 2.66 Å, Ba<sup>2+</sup> 2.70 Å, NH<sub>4</sub><sup>+</sup> 2.84 Å, Cs<sup>+</sup> 3.34 Å.

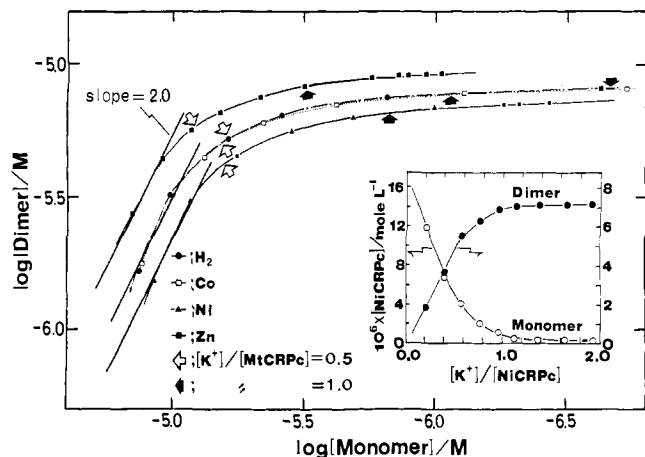
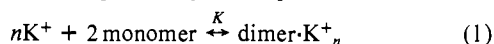


**Figure 3.** Plots of  $\log$  [monomer] versus  $\log$  [dimer] for several MtCRPc in  $\text{CHCl}_3$  solution. Experimental data as appeared in Figure 1 were analyzed with a computer program based on the approximation method of West and Pearce.<sup>16</sup> The solid lines are drawn with the theoretical slope of 2. The inset shows the dependence of monomer and/or dimer concentration of NiCRPc on  $[\text{K}^+]/[\text{NiCRPc}]$  calculated for our experimental system.

phthalocyanines<sup>13</sup> shows that the loss of low-energy Q-band absorption, near 660–700 nm, of the monomeric species and the shift to a broad absorption near 620–640 nm are consistent with electronic coupling between a pair (or more) of phthalocyanine units. In this case, as will be documented more fully below, dimerization is the exclusive process.

From the plot (Figure 2) of the intensity changes with  $[\text{K}^+]$ , there is evidence for a two-step three-stage process. The first, second, and third stages occur approximately at  $[\text{K}^+]/[\text{MtCRPc}]$  values of 0–0.5, 0.5–1.5, and over 1.5, respectively. The  $\text{K}^+$ -induced two-step three-stage process is also obvious from the shift in position of the isobestic points (Figure 1).<sup>15</sup>

Assuming the monomer–dimer equilibrium (eq 1) for the  $\text{K}^+$ -triggered spectroscopic change, the specific monomer and



dimer concentrations were derived with use of the method of West and Pearce,<sup>16</sup> using as data the changes of intensity at two wavelengths, as a function of  $[\text{K}^+]$ . The pure monomer spectrum<sup>17</sup> was assumed to be present in the absence of  $\text{K}^+$ . With use of this procedure, proof of formation of the dimer may be obtained by plotting the calculated  $\log$  [monomer] against calculated  $\log$  [dimer].<sup>18</sup> A slope of 2 will be obtained if eq 1 is applicable. Formation of higher oligomers would cause the slope to be more steep than 2. Indeed as revealed in Figure 3 there is a region where the slope is 2.0. When  $\text{K}^+$  ions are added to a MtCRPc solution, the monomer concentration decreases sharply, and a region with slope = ca. 2.0 continues until  $[\text{K}^+]/[\text{MtCRPc}] = 0.5$ . After this point, the slope of the plot approaches zero, especially beyond the region  $[\text{K}^+]/[\text{MtCRPc}] \geq 1.0$ .

Thus the monomer–dimer conversion proceeds with a very high formation constant ( $K$  for eq 1 with  $n = 1$ ,  $(6 \pm 2) \times 10^9 \text{ L}^2 \text{ mol}^{-2}$ ) until two MtCRPc units bind one cation. Subsequently the spectroscopic changes in the  $[\text{K}^+]/[\text{MtCRPc}] \geq 1.0$  region are no longer a monomer-to-dimer transformation process but, rather, rearrangement of one form of dimer to another. The region  $0.5 \leq [\text{K}^+]/[\text{MtCRPc}] \leq 1.5$  can be considered to be the transition stage where the MtCRPc–cation–MtCRPc complex combines with

(15) The shift in the position of the isobestic points was most clearly observed for the CuCRPc and NiCRPc system. For the CuCRPc system, the isobestic points of the 1st and 2nd stages appeared at 370 and 641 nm, while those for the 2nd and 3rd emerged at ca. 418 and 665 nm. For NiCRPc, isobestic points were similarly observed at 378 and 632 nm, and at 404 and 672 nm, respectively.

(16) Pearce, S.; West, W. *J. Phys. Chem.* **1965**, *69*, 1894.

(17) Judging from the previously accumulated data,<sup>3</sup> spectra of MtCRPcs in  $\text{CHCl}_3$  are clearly those of monomer at  $[\text{MtCRPc}] < 2 \times 10^{-5} \text{ M}$ .

(18) Nevin, W. A.; Liu, W.; Lever, A. B. P. *Can. J. Chem.* **1987**, *26*, 891.

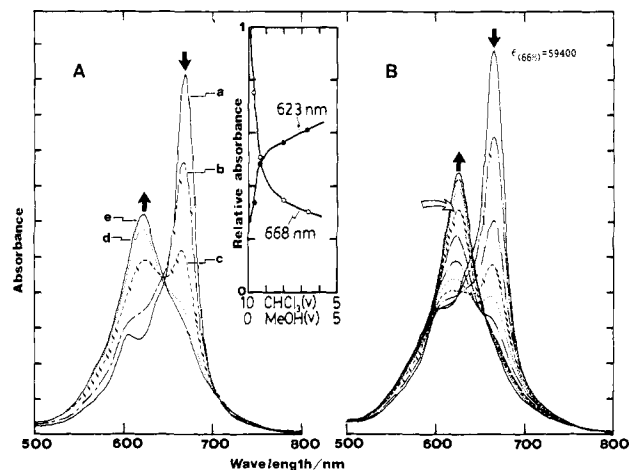


**Figure 4.** (A) Absorption spectra of CoCRPc in  $\text{CHCl}_3$ –MeOH mixtures: (a)  $\text{CHCl}_3$  alone, (b)  $\text{CHCl}_3$ :MeOH = 2.9:0.1 (v/v), (c)  $\text{CHCl}_3$ :MeOH = 2.8:0.2 (v/v), (d)  $\text{CHCl}_3$ :MeOH = 2.4:0.6 (v/v), (e)  $\text{CHCl}_3$ :MeOH = 2.0:1.0 (v/v). (B) Change in absorption spectrum of CoCRPc by the addition of  $\text{CH}_3\text{COOK}$ . Experiments were carried out as described for Figure 1. The spectrum shown by an open arrow was recorded at  $[\text{K}^+]/[\text{CoCRPc}] = 1.63$ .

a 2nd and 3rd cation. Considering that the blue shift in the Q and Soret absorption in the dimers can be explained by an exciton interaction<sup>19</sup> and that the ESR data for CuCRPc in the presence of  $\text{K}^+$  or  $\text{Ca}^{2+}$  (vide infra) will indicate the presence of two copper atoms in very close proximity, the last stage ( $[\text{K}^+]/[\text{MtCRPc}] \geq 1.5$  in Figure 2) can be ascribed to cofacial complex formation. Thus after formation of a non-cofacial MtCRPc–cation–MtCRPc dimeric complex, increasing cation concentration causes a conformational change in the dimer wherein the two phthalocyanine halves encapsulate two or more cations leading to the formation of the cofacial dimer, i.e., a supermolecular phthalocyanine is attained. Probably encapsulation continues until the available sites are saturated, i.e., until two MtCRPc units bind four cations in a rigid eclipsed dimer. The inset of Figure 3 shows the calculated monomer and dimer concentrations of NiCRPc as a function of  $[\text{K}^+]/[\text{NiCRPc}]$ . Although not shown, similar behavior is observed with the other MtCRPc species; thus dimerization is essentially complete (but not cofacial dimerization) when  $[\text{K}^+]/[\text{MtCRPc}] > 1.0$ .

The addition of sodium ions did lead to a change in spectrum (Figure 1B) in contradistinction to the porphyrin series.<sup>7a</sup> The band due to the monomer species decreases in intensity, while there is growth in the band due to the dimeric species. Sodium ions are, however, unable to effect the complete conversion to a spectrum, obtained with potassium ions, typical of the cofacial species.

(ii) **Solvent-Induced Dimerization.** The intensity of the MtCRPc Q band peak (around 660–700 nm) decreases if the solvent is changed from chloroform to methylene chloride, benzene, DMF, dimethyl sulfoxide, toluene, THF, ethyl acetate, methanol, etc. In such circumstances the change in spectrum exactly parallels that observed upon  $\text{K}^+$  addition. Such spectroscopic changes are also observed in mixed solvents, e.g., Figure 4A shows the effect of mixing methanol into chloroform upon the CoCRPc spectrum. With increasing ratio of methanol to chloroform, the peak height at 668 nm (mainly monomer) decreases but that at 625 nm (mainly dimer) increases. For comparison, Figure 4B shows the corresponding data for addition of  $\text{K}^+$ . The dimeric spectrum induced by the methanol solvent ( $\text{CHCl}_3$ :MeOH = 2:1 (v/v)) is essentially identical with that obtained at a  $[\text{K}^+]/[\text{CoCRPc}] = 1.6$  ratio which demonstrates that the mixed solvent is giving rise to cofacial dimer formation. Unfortunately the very low solubility of the metalated crown phthalocyanines in dimer-forming solvents (ca.  $1 \times 10^{-5} \text{ M}$ ) precludes other methods of characterization.

(19) Kasha, M.; Rawls, H. R.; Et-Bayoumi, M. A. *Pure Appl. Chem.* **1965**, *11*, 371.

**Table III.** Magnetic Parameters<sup>24</sup> of Cation-Induced CuCRPc Cofacial Dimers<sup>a</sup>

compd	$g_1$	$g_2$	$A_{1\parallel}$ , G	$A_{1\perp}$ , G	$D_1$ , G	$D_2$ , G	freq, MHz	Cu-Cu <sup>b</sup> dist, Å
[CuCRPc] <sub>2</sub> (K <sup>+</sup> ) <sub>4</sub>	2.050	2.152	107	103	371	407	9093	4.2
[CuCRPc] <sub>2</sub> (Ca <sup>2+</sup> ) <sub>4</sub>	2.047	2.141	105	104	375	425	9096	4.1

<sup>a</sup> See Figure 5 for definition of parameters. <sup>b</sup> Calculated via  $r^3 = (1.39 \times 10^4) \times g_2/D_2$ , where  $D$  is in G and  $r$  is in Å.<sup>24</sup>

Note that the solubility of the monomers in chloroform is several orders greater.

(iii) **Electron Spin Resonance.** Of the several MtCRPc species investigated, CuCRPc is expected to provide the most definitive ESR spectra. Preliminary studies showed that data collection in a chloroform-methanol mixture provided better data than that in pure chloroform. The spectrum of CuCRPc obtained in the absence of any cations (Figure 5A) is structureless and seems to be that of a somewhat aggregated species.<sup>20</sup>

Addition of an excess of sodium ions led to the development of a well-defined structured signal (Figure 5B-a) in frozen solution, basically very similar to previously observed monomeric copper porphyrin and phthalocyanine species, e.g., copper(II) tetraphenylporphyrin.<sup>21</sup> The spectrum is clearly axial and contains both copper hyperfine and nitrogen (from the four coordinating phthalocyanine nitrogen atoms) super-hyperfine structure. The parameters ( $g_{\parallel} = 2.166$ ,  $g_{\perp} = 2.049$ , and  $A_{\parallel}^{\text{Cu}} = 228 \times 10^{-4}$ ,  $A_{\perp}^{\text{N}} = 16.7 \times 10^{-4}$ ,  $A_{\parallel}^{\text{N}} = 14.3 \times 10^{-4} \text{ cm}^{-1}$ ) are typical values for a species of this type. As developed further below, the solution giving rise to this spectrum contains about 50% mononuclear species and 50% of the non-cofacial dimer almost certainly with sodium ions occupying the ether voids in both cases. In the absence of sodium ions, the solution is partially aggregated, resulting in broadening of the resonance signals. In the presence of sodium ions, the resulting positive charge keeps the copper atoms separated and a clean highly resolved ESR spectrum is observed.

Dramatic changes in the ESR spectrum of CuCRPc occur when K<sup>+</sup> or Ca<sup>2+</sup> ions are added (Figure 5C,D). This observation differs from the corresponding Cu(II) crown porphyrin where K<sup>+</sup>, but not Ca<sup>2+</sup>, was effective.<sup>7a</sup> Thus with CuCRPc both cations yield two strong perpendicular transitions in the  $g = 2$  region. These transitions do not exhibit nitrogen super-hyperfine coupling but do show the characteristic seven-line pattern expected for two equivalent Cu(II) ions coupled together.<sup>22</sup> In the half-field region ( $\Delta M = \pm 2$ ), seven equally spaced lines (87–88 G separation) are observed. These data provide unmistakable evidence for the formation of a symmetric dimeric molecule. The absence of any ESR signal originating from a monomeric CuCRPc molecule, under these conditions, attests to a high formation constant. Moreover the overall band envelope is essentially identical with those of various well-defined symmetric binuclear and coupled copper complexes in the literature.<sup>23</sup> The data in spectra C and D of Figure 5 also exclude any significant proportion of higher aggregate.

The ESR parameters for these spectra are collected in Table III, having been evaluated by standard procedures.<sup>24</sup> Most importantly it is possible to evaluate the Cu-Cu distance from the zero field splitting parameters.<sup>25</sup> In this fashion the calculated

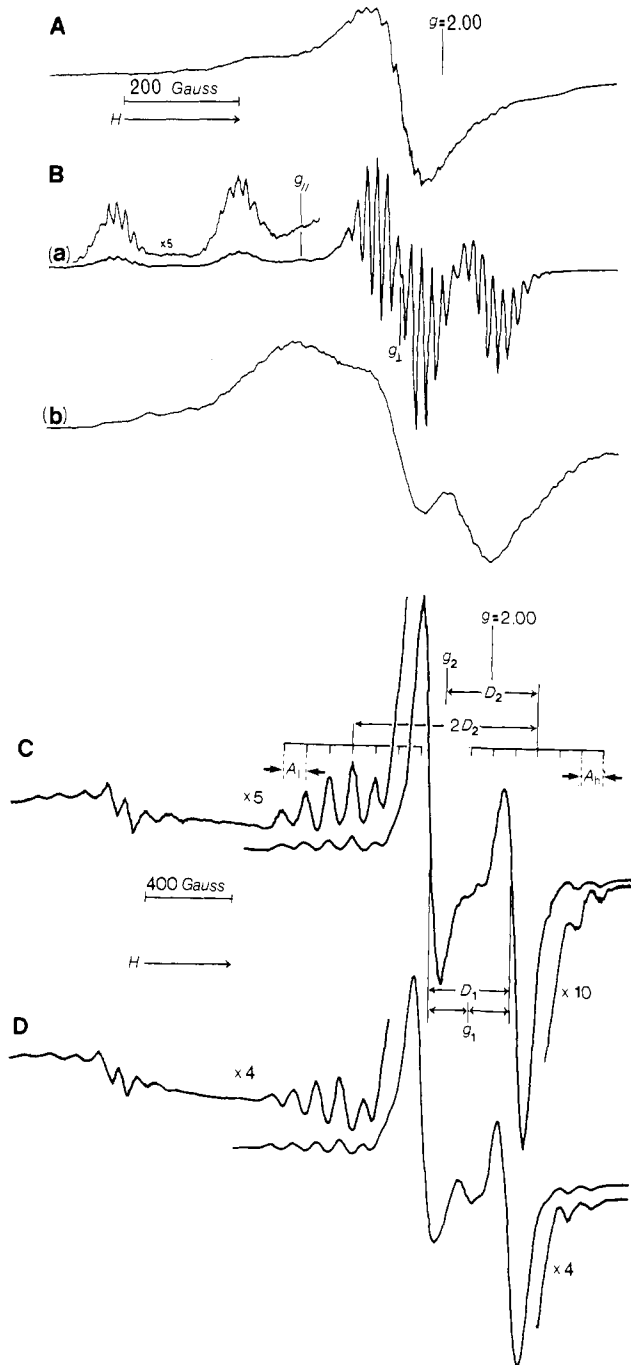


**Figure 5.** ESR spectra of CuCRPc in CHCl<sub>3</sub>-MeOH (ca. 4:1 (v/v)): (A) in the absence of any cation and in the presence of (B) saturated CH<sub>3</sub>COONa at (a) 77 K and (b) room temperature, (C) CH<sub>3</sub>COOK, ([K<sup>+</sup>]/[CuCRPc] = 4), and (D) CaCl<sub>2</sub> ([Ca<sup>2+</sup>]/[CuCRPc] = 10). [CuCRPc] = 1 mM.

Cu-Cu distance is found to be ca. 4.1 Å, in the presence of K<sup>+</sup> or Ca<sup>2+</sup>. This is nearly identical with the distance estimated from CPK molecular models.<sup>26</sup> Note that in the presence of ammonium ions, dimerization does occur and two strong perpendicular

(20) Skorobogaty, A.; Smith, T. D.; Dougherty, G.; Pilbrow, R. *J. Chem. Soc., Dalton Trans.* **1985**, 651 and several references cited therein.

(21) Manoharan, P. T.; Rogers, M. T. In *Electron Spin Resonance of Metal Complexes*; Yen, T. F., Ed.; Plenum: New York, 1979.

(22) Smith, T. D.; Pilbrow, J. R. *Coord. Chem. Rev.* **1974**, *13*, 173. Eaton, S. S.; More, K. M.; Sawant, B. M.; Boymel, P. M.; Eaton, G. R. *J. Magn. Reson.* **1983**, *52*, 435. Thomson, C. Q. *Rev. Chem. Soc.* **1968**, *22*, 45. Kottis, P.; Lefebure, R. *J. Chem. Phys.* **1963**, *39*, 393.

(23) (a) Eaton, S. S.; More, K. M.; Sawant, B. M.; Eaton, G. R. *J. Am. Chem. Soc.* **1983**, *105*, 6560. (b) Eaton, S. S.; Eaton, G. R.; Chang, C. K. *Ibid.* **1985**, *107*, 3117. (c) Chang, C. K. *J. Heterocycl. Chem.* **1977**, *14*, 1285. (d) Eaton, S. A.; Eaton, G. R. *J. Am. Chem. Soc.* **1982**, *104*, 5002.

(24) Chikira, M.; Yokoi, H.; Isobe, T. *Bull. Chem. Soc. Jpn.* **1974**, *47*, 2208. Chikira, M.; Kon, H.; Hawley, R. A.; Smith, K. M. *J. Chem. Soc., Dalton Trans.* **1979**, 246 and some references cited therein. Chasteen, N. D.; Belford, R. L. *Inorg. Chem.* **1970**, *9*, 169.

(25) It is possible to estimate the Cu-Cu distance from the ratio of the intensity of the forbidden half-field transition ( $\Delta M = \pm 2$ ) to the intensity of the allowed transitions ( $\Delta M = \pm 1$ ).<sup>23a,b,d</sup> In our case, this ratio is  $4.1 \times 10^{-3}$ , which corresponds to  $r = 4.15$  Å.

(26) The crystal structure of benzo-15-crown-5 reveals that the plane containing ether oxygens makes an angle of 31° with the benzene ring; Hanson, I. R. *Acta Crystallogr., Sect. B* **1978**, *B34*, 1026.

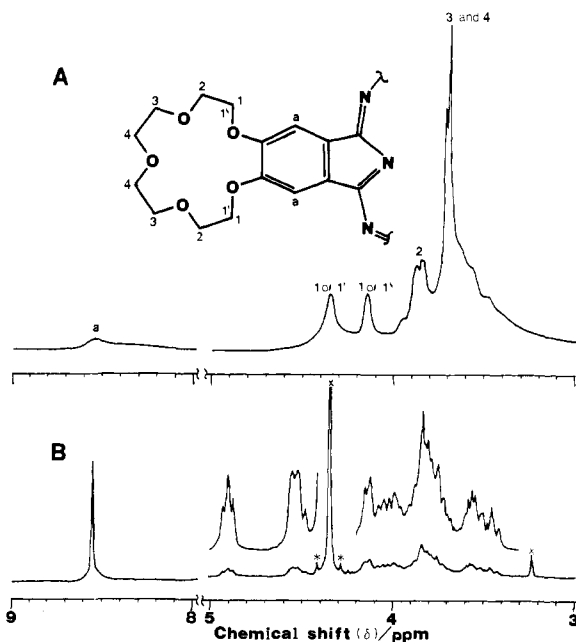


**Figure 6.** 300-MHz proton NMR spectra of ZnCRPc in (A)  $\text{CDCl}_3$  and (B)  $\text{CDCl}_3$  containing a trace amount of  $\text{CD}_3\text{OD}$  in the presence of  $\text{CaCl}_2$ . Signals marked  $\times$  and  $*$  are due to solvents.

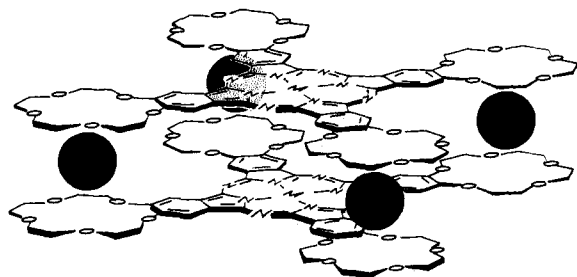


**Figure 7.** A proposed structure for the cation-induced dimer of MtCRPc. Solid circles indicate cations such as  $\text{K}^+$  and  $\text{Ca}^{2+}$ .

transitions are observed, but the seven-line pattern is not resolved.

(iv)  $^1\text{H}$  NMR Spectra. The  $^1\text{H}$  NMR spectrum of ZnCRPc is shown in Figure 6, in both the presence and the absence of cations. The spectrum of mononuclear ZnCRPc is complex, in the high-field region, due to a large number of chemically inequivalent ether fragments, but the signals are well separated by the ring current anisotropy of the phthalocyanine core. Assignments are shown in Figure 6.

The addition of  $\text{CaCl}_2$  to a solution of ZnCRPc ( $[\text{Ca}^{2+}]/[\text{ZnCRPc}]$  ca. 10) increases the complexity of the high-field region (Figure 6B) and the signals spread out, especially downfield. These data are consistent with cofacial dimer formation (Figure 7). The singlet of aromatic protons does not significantly shift but becomes sharper, due probably to the restricted rotation of the  $\text{O}-\text{CH}_2-\text{CH}_2-\text{O}$  groups or to the greater rigidity imposed by encapsulation of the cations. The negligible shift of the singlet is expected since the 3,4-protons of one phthalocyanine fall in the "black region" of the anisotropic shielding effect of the second ring,<sup>27</sup> assuming the interplanar distance is close to  $4.1 \text{ \AA}$ .<sup>28</sup>

The pyrrole protons of  $\text{H}_2\text{CRPc}$  shift from  $-3.41$  to  $-8.09$  ppm with cofacial dimer formation consistent with the structure in Figure 7. This large upfield shift indicates an intense diamagnetic ring current interaction in this dimer.<sup>29</sup>

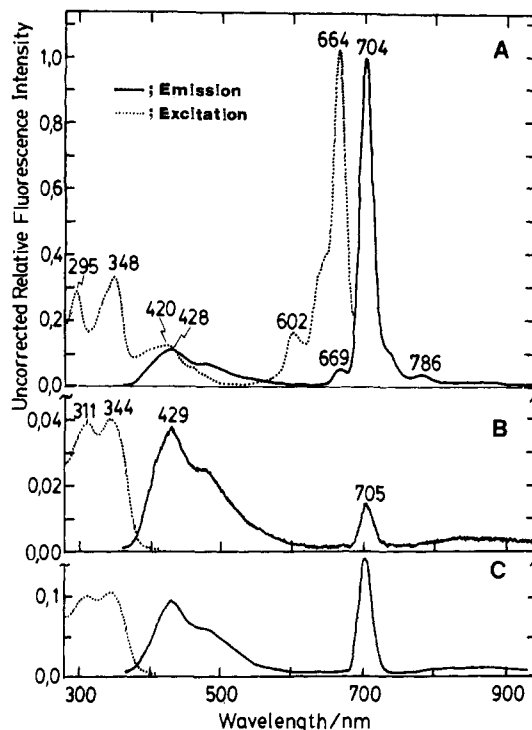


**Figure 8.** Emission and excitation spectra of  $\text{H}_2\text{CRPc}$  (A) in  $\text{CHCl}_3$  (emission excited at  $350 \text{ nm}$ ), (B) in the presence of  $\text{CH}_3\text{COOK}$  in  $\text{CHCl}_3$  containing  $0.1 \text{ v/v}$  percent of  $\text{MeOH}$ , and (C) in the presence of  $\text{CH}_3\text{COONa}$  in  $\text{CHCl}_3$  containing  $0.1 \text{ v/v}$   $\text{MeOH}$ .  $[\text{H}_2\text{CRPc}]/M = 4.91 \times 10^{-6}$ .  $[\text{CH}_3\text{COOK}]/[\text{H}_2\text{CRPc}] = 2.62$ .  $[\text{CH}_3\text{COONa}]/[\text{H}_2\text{CRPc}] = 98$ . Excitation spectra were recorded for emission peaks at (A)  $704 \text{ nm}$ , (B)  $429 \text{ nm}$ , and (C)  $429 \text{ nm}$ .

(v) **Emission Spectroscopy.** Fluorescent emission from the lowest  $\pi-\pi^*$  (Q band) state is common in metal-free, zinc, and other main group phthalocyanines.<sup>30,31</sup> Both mononuclear  $\text{H}_2\text{CRPc}$  and  $\text{ZnCRPc}$  exhibit such emission near  $700 \text{ nm}$ . The excitation spectrum of this emission (Figure 8A) parallels that of other mononuclear phthalocyanines<sup>13</sup> except for a rather prominent excitation near  $430 \text{ nm}$  which is also observed in absorption (Table II). This is rather unusual for a phthalocyanine unit and may involve the ether oxygen lone pairs.

Emission from the upper excited  $\pi-\pi^*$  state (Soret), so-called  $\text{S}_2$  emission, is not uncommon in porphyrin chemistry.<sup>32-34</sup> We have recently noted that several binuclear and tetranuclear phthalocyanines also exhibit upper excited state emission<sup>35</sup> and also find that both metal-free and zinc crown phthalocyanine monomer species exhibit emission in chloroform near  $430 \text{ nm}$

(30) Gouterman, M. In *The Porphyrins*; Dolphin, D., Ed; Academic: New York, 1978; Vol. III, p 1. Gouterman, M. *J. Chem. Phys.* **1959**, *30*, 1139; **1960**, *33*, 1523.

(31) Vincent, P. S.; Voigt, E. M.; Rieckhoff, K. E. *J. Chem. Phys.* **1971**, *55*, 4131.

(32) Bajema, L.; Gouterman, M. *J. Mol. Spectrosc.* **1971**, *39*, 421. Zaleski, I. E.; Kotlo, V. N.; Sevchenko, A. N.; Solov'ev, K. N.; Shkirman, S. F. *Sov. Phys. Dokl.* **1973**, *18*, 320; **1975**, *19*, 589. Fielding, P. E.; Mau, A. W.-H. *Aust. J. Chem.* **1976**, *29*, 933. Avakiss, J.; Freiberg, A.; Savikhin, S.; Stelmakh, G. F.; Tsvirko, M. P. *Chem. Phys. Lett.* **1984**, *111*, 275.

(33) In the porphyrin system, cofacial dimer units emit more weakly than monomer: Kagan, N. E.; Mauzerall, D.; Merrifield, R. B. *J. Am. Chem. Soc.* **1977**, *99*, 5486. Chang, C. K.; Kuo, M.-S.; Wang, C.-B. *J. Heterocycl. Chem.* **1977**, *14*, 943. Chang, C. K. *Ibid.* **1977**, *14*, 1285. Guckel, F.; Schweiser, D.; Collman, J. P.; Bencosme, S.; Evtitt, E.; Sessler, J. *Chem. Phys.* **1984**, *86*, 161. Mialoco, C.; Glannotti, A.; Mallard, P.; Momeuteau, M. *Chem. Phys. Lett.* **1984**, *112*, 87.

(34) Ohno, O.; Kaisu, Y.; Kobayashi, H. *J. Chem. Phys.* **1985**, *82*, 1779. Kaizu, Y.; Maekawa, H.; Kobayashi, H. *J. Phys. Chem.* **1986**, *90*, 4234. Selensky, R.; Holten, D.; Windsor, M. W.; Paine, J. B., III; Dolphin, D. *Chem. Phys.* **1981**, *60*, 33. Brookfield, R. L.; Ellul, H.; Harriman, A.; Porter, G. *J. Chem. Soc., Faraday Trans. 2* **1986**, *82*, 219. Kurabayashi, Y.; Kikuchi, H.; Kokubun, H.; Kaizu, Y.; Kobayashi, H. *J. Phys. Chem.* **1984**, *88*, 1308.

(35) Mannivannan, V.; Kobayashi, N.; Nevin, W. A.; Seymour, P.; Lever, A. B. P.; Leznoff, C. C., unpublished data.

(27) Janson, T. R.; Kane, A. R.; Sullivan, J. F.; Knox, K.; Kenney, M. E. *J. Am. Chem. Soc.* **1969**, *91*, 5210. Kane, A. R.; Yalman, R. G.; Kenney, M. E. *Inorg. Chem.* **1968**, *7*, 2558. Esposito, J. N.; Lloyd, J. E.; Kenney, M. E. *Ibid.* **1966**, *5*, 1979.

(28) Johnson, C. E.; Bovey, F. A. *J. Chem. Phys.* **1958**, *29*, 1012.

(29) Satterlee, J. D.; Shelnut, J. A. *J. Phys. Chem.* **1984**, *88*, 5487.

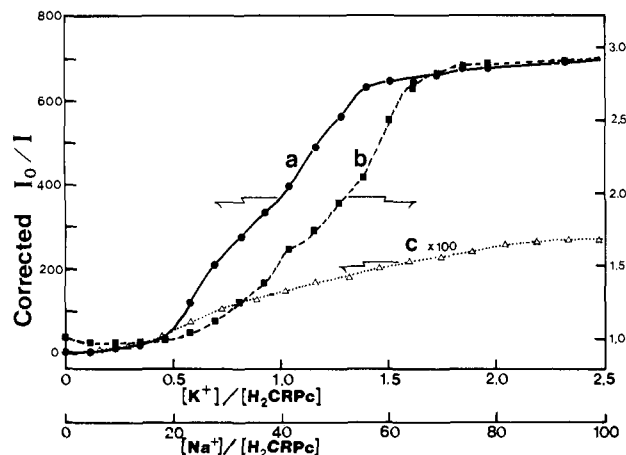


Figure 9. Stern-Volmer plots of the emission of  $H_2CRPc$ : (a)  $S_1$  emission quenched by  $K^+$  ion; (b)  $S_2$  emission quenched with  $K^+$  ion; (c)  $S_2$  emission quenched with  $Na^+$  ion.

(Figure 8). These are the first examples of phthalocyanine upper excited state emission.

The crown  $S_2$  emission is broader than the  $S_1$  emission and the band shape is similar to that observed for tetraazaporphyrin free base and its zinc derivative.<sup>32</sup> The excitation spectra of the  $S_2$  emission is similar, but not identical, to the  $S_1$  excitation spectra (Figure 8A; Table II). Assuming that the  $S_2$  emission originates in the same transition which gives rise to the well-developed 420-nm absorption, then the Stokes shift for  $S_2$  emission is, as in the porphyrin species, very small.

By using the known quantum yields of quinine sulfate<sup>8a,b</sup> (for  $S_2$ ) and free-base tetraphenylporphyrin<sup>8c</sup> for calibration, the quantum yields for  $S_1$  and  $S_2$  emission were determined to be, in chloroform, 0.7 and  $1 \times 10^{-2}$  for  $H_2CRPc$ . Some solution instability precluded an accurate determination for ZnCRPc. The  $S_1$  quantum yield is very similar to those observed earlier for unsubstituted metal-free and zinc phthalocyanine species.<sup>30,31</sup>

Addition of  $K^+$  to metal-free and zinc crown Pc monomers in chloroform (concentration  $< 5 \times 10^{-6}$  M) leads to quenching of both the  $S_1$  and  $S_2$  emission, in a parallel fashion (Figure 8B). The concentration of  $K^+$  ion required to quench the fluorescence intensity of a crowned porphyrin is apparently very much less than the concentration of the cation required to reduce the optical density of the porphyrin in the ground state.<sup>7a</sup> In the crown phthalocyanine system (Figure 9), on the other hand, the quenching behavior corresponds almost exactly to that in the absorption study (Figure 2). The Stern-Volmer plot for  $S_1$  emission (Figure 9a) is clearly consistent with stepwise encapsulation of the  $K^+$  ions. In the  $0 < [K^+]/[H_2CRPc] < 0.5$  region where the non-cofacial  $H_2CRPc-K^+-H_2CRPc$  species forms (Figures 2 and 3), quenching is not marked, though it does occur to a small degree. However, with further increase in  $[K^+]$ , quenching is greatly enhanced while above  $[K^+]/[H_2CRPc] = ca. 1.5$  the emission intensity become almost constant. The residual emission intensity has an excitation spectrum identical with that of the monomer species and an intensity about 1/700 of the initial intensity. It is due to the small amount of monomer species in equilibrium with the cofacial species, implying that the cofacial dimer does not emit.<sup>33</sup>

The quenching of the  $S_2$  emission parallels that of the  $S_1$  quenching except that the degree of quenching is much less marked (Figure 9b). There is also some remaining  $S_2$  emission that appears to arise from the cofacial dimer since it is relatively very much more intense than can be reconciled with the equilibrium monomer content (intensity 2/5 of initial value, upon cofacial dimer formation) (Figure 9b). However, the excitation spectrum of this residual  $S_2$  emission is the same as in the monomeric species. There remains the suspicion that the  $S_2$  emission does not indeed originate from the phthalocyanine but from an impurity. This possibility appears excluded by the similarity of its excitation spectrum to the Soret absorption and the similarity of its quenching

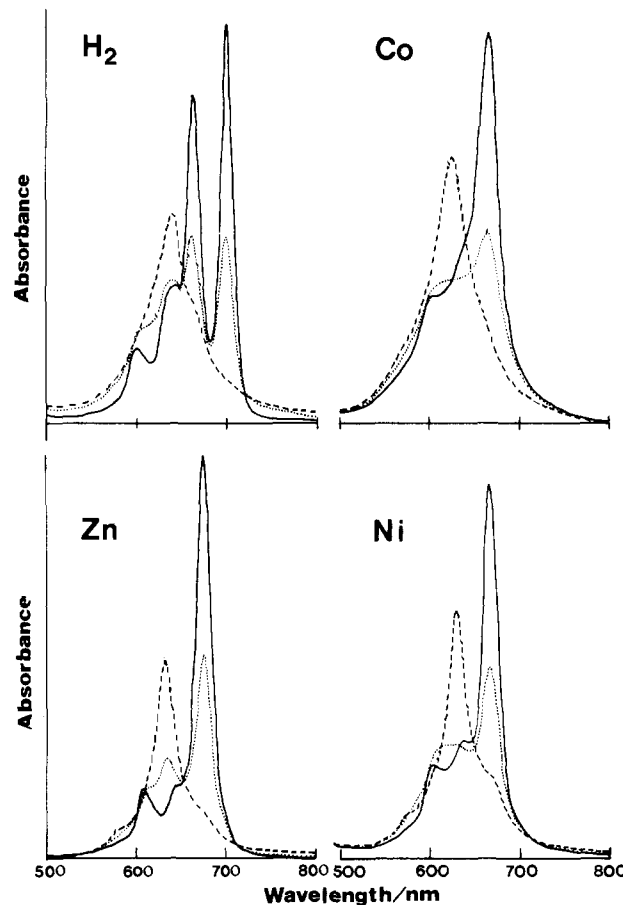


Figure 10. Absorption spectra of several MtCRPc species as indicated. Monomeric species (—) (in chloroform), cofacial  $[MtCRPc]_2K^+_4$  species (---) (in chloroform with 0.1% methanol), and solutions with  $[K^+]/[MtCRPc] = 0.5$  containing a roughly 50:50 mixture of monomeric and non-cofacial  $[MtCRPc]-K^+-[MtCRPc]$  species (···) (in chloroform with 0.02% methanol).

behavior to that of  $S_1$ , but, as noted above, there are some inconsistencies.

The addition of  $Na^+$  ion to a chloroform  $H_2CRPc$  solution also quenches, to some degree, both the  $S_1$  and  $S_2$  emission (Figure 9c). However, much higher concentrations of  $Na^+$  are needed and it is clearly much less efficient. In the crown porphyrin case,<sup>7a</sup>  $Na^+$  did not perturb emission. As indicated above,  $Na^+$  ion only takes the species to the second non-cofacial dimer stage.

(vi) Absorption Spectra (Table II). (a) Mononuclear Species and Cofacial Dimer. The mononuclear species have absorption spectra in chloroform (Figure 2; Table II) typical of mononuclear MtPc species<sup>3</sup> though with a prominent shoulder or peak near 420 nm which is not so common. Its appearance is reminiscent of the hyper-porphyrin spectra, showing similar additional absorption, but the latter arises as a consequence of the central ion having an  $(np)_2^2$  pair of electrons, e.g., Pb(II).<sup>30</sup> This 420-nm band shifts but does not disappear upon cofacial dimer formation.

The formation of the cofacial dimeric species provides a convenient method of studying exciton coupling in an eclipsed phthalocyanine species. Some spectra of fully eclipsed cofacial species are shown in Figure 10, and the data are collected in Table II. Not that under the conditions  $[K^+]/[MtCRPc] > 1.5$ , the quantity of mononuclear species in equilibrium with the cofacial dimer is less than 0.2% and therefore its spectrum makes no significant contribution to the spectra reported here for the cofacial species. The most interesting feature of the cofacial dimeric spectra is the single rather broad (compared to the monomer) and symmetrical Q band absorption. Although the molar extinction coefficients of the cofacial dimer Q bands are approximately one-half of the corresponding monomer Q bands, the oscillator strengths are essentially identical, i.e., there is no loss in transition

probability in forming the dimer (see Table II).

Thus exciton coupling of the two  $Q S_1$  states leads to two new levels corresponding to an in-phase and out-of-phase coupling. Transitions to the lower, out-to-phase, component are forbidden rigorously in an eclipsed  $D_{4h}$  species.<sup>36</sup> For compounds that show typical monomeric and dimeric spectra (MtCRPc,  $M = \text{Zn, Cu, Ni, Co}$ ), the Q band blue shift upon dimerization is about 880–980  $\text{cm}^{-1}$ . For parallel eclipsed dimers with negligible distortion from  $D_{4h}$  symmetry, the dipole–dipole excitation splitting,  $V$ , is given by eq 2<sup>37</sup>

$$V = e^2 M^2 / 4\pi h c \epsilon_0 R^3 \quad (2a)$$

$$= (1.16 \times 10^5) M^2 / R^3 \quad (2b)$$

where  $M$  and  $R$  are the dipole length, and the inter-molecular separation, respectively,  $\epsilon_0$  is the permittivity in a vacuum, and the other parameters have their usual meaning.  $V$  is given in wavenumbers in (2b) if  $M$  and  $R$  are expressed in Å. The dipole length in Å can be estimated from eq 3<sup>30</sup>

$$M^2 = (\epsilon_{\text{max}} / 2513G)(\Delta\lambda / \lambda) \quad (3)$$

where  $G$  is the degeneracy, 2 in this case,  $\Delta\lambda$  is the half-bandwidth,  $\lambda$  is the wavelength, and  $\epsilon_{\text{max}}$  is the molar extinction coefficient of the dimer Q band, respectively. In this fashion the  $M$  values are estimated to be about 0.68–0.98 Å. Alternatively  $M$  may be estimated from the oscillator strength<sup>38</sup> yielding the same result. Assuming a distance of  $R = 4.1$  Å, from ESR, the exciton splitting is calculated to be about 770–1600  $\text{cm}^{-1}$ . The exciton splitting may also be estimated as twice the energy difference between the mononuclear Q band and dimeric Q band peak energies, yielding about 1760, 1960, 1910, and 1960  $\text{cm}^{-1}$  for Ni, Co, Cu, and ZnCRPcs, respectively. This compares with an exciton splitting of about 2500  $\text{cm}^{-1}$  for the binuclear bridged cofacial phthalocyanine species.<sup>13</sup> Using these data and eq 3 provides an alternate route to estimating inter-metallic distances; the electronic spectra and electron spin resonance experiments yield comparable results.

The Soret band is much less obviously affected by formation of the cofacial dimer. There is generally a small blue shift but little change in intensity. Nevertheless the shift is comparable to that seen in the Q band.<sup>5a</sup> Thus coupling of the Soret states does appear to have taken place even though little quenching of the  $S_2$  emission apparently occurs.

**(b) Non-cofacial Dimer.** The spectra of the non-cofacial dimer, obtained with  $[\text{K}^+]/[\text{MtCRPc}] = 0.5$ , are collected in Figure 10, while the spectrum of the sodium ion induced non-cofacial dimer of CuCRPc is shown in Figure 1, in both cases in admixture with the mononuclear species. With  $[\text{K}^+]/[\text{MtCRPc}] = 0.5$ , there is approximately 50% of monomeric species in equilibrium with the non-cofacial dimer. In Figure 11 the spectra of several non-cofacial dimeric species are shown, obtained by subtracting the spectrum of the mononuclear species from the admixed spectra. One observes that the resulting spectrum is very similar to that of the cofacial species and with an intensity, per dimeric unit, slightly less than that of the cofacial dimer. There is also evidence for the existence of a new shoulder or peak to the blue of the main Q band absorption, and little evidence for any additional absorption to the red of the Q dimer peak. There is no shifting in the Soret band (Figure 1).

The initial non-cofacial dimer, second stage product, reasonably consists of a dimeric molecule whose two halves are joined together at one ether unit by a bridging potassium ion. In fluid solution there may be many conformational forms of this dimeric unit. The electronic spectrum will consist of a "snap-shot" of all possible conformations. If there is free rotation about the potassium ion,

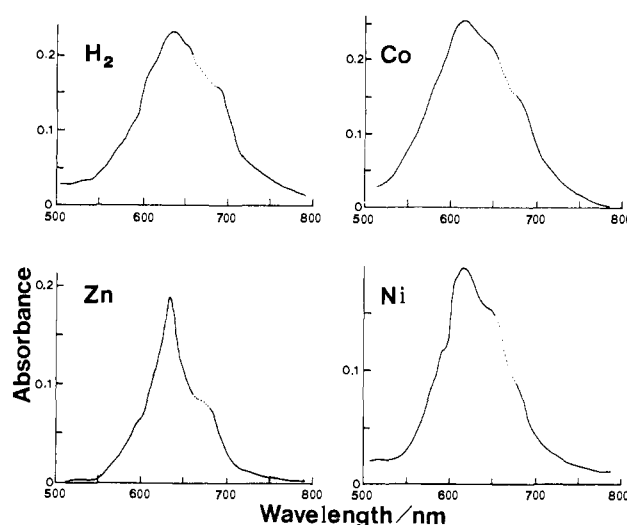


**Figure 11.** Estimated spectra of several non-cofacial  $[\text{MtCRPc}]\text{-K}^+$   $[\text{MtCRPc}]$  species obtained from data in Figure 10 by subtraction of the monomeric component. The spectra in the region of the dotted lines are approximate due to uncertainty in the amount of monomeric species to subtract (ca. 40–50%).

then many conformational forms will have symmetry much lower than  $D_{4h}$ . Such a situation will give rise to substantial absorption to the red of the cofacial dimeric peak,<sup>18,36</sup> yet this does not appear to be observed, rather, additional absorption is seen to the blue. Suppose instead that the ether voids, which are rather bulky, inhibit such rotation and restrict the molecule to an end-to-end stretched out  $180^\circ$  conformation of  $C_{2h}$  symmetry, viewed edgewise-on as a step conformation. Such a conformation would show two higher energy peaks due to the splitting of the otherwise degenerate exciton coupled state, but transitions to the two lower energy states remain strictly forbidden.<sup>36</sup> Thus the data appear to support such a linear step conformation. Recall, further, that the ESR spectrum of the  $\text{CuCRPc}\text{-Na}^+\text{-CuCRPc}$  solution shows no evidence for Cu–Cu coupling, consistent with the stretched out formulation.

Note further that the two parts of the step must be parallel—if their angle were greater than  $180^\circ$ , i.e., they were tilted away from each other, absorption to the red of the dimer peak would be expected. Such tilting must be absent or small.

It is noteworthy that the mononuclear emission from  $S_1$  is not quenched to any significant extent upon formation of the stage 2 non-cofacial dimer irrespective of whether it is potassium or sodium ion induced. Since the electronic spectra of these species show significant electronic coupling effects, such an observation is rather surprising.

### Concluding Remarks

The structure of the final stage 3 dimeric species, assigned to a fully eclipsed cofacial  $D_{4h}$  dimer, is required when we assume that the two halves are held together by potassium ions bridging crown ether units. With four  $\text{K}^+$  ions shared by two MtCRPc units, a parallel arrangement of the Pc planes can surely be anticipated. This structure is supported by the Cu ESR spectrum, by the presence of a single very symmetric, rather weak, and rather narrow Q absorption band (compared with the half-bandwidths for more flexible binuclear phthalocyanine species), by the emission, and also by the NMR spectra. Note, too, that the cofacial free base  $[\text{H}_2\text{CRPc}]_2\text{K}^+_4$  species also possesses a single relatively narrow Q band absorption suggesting it too possesses  $D_{4h}$  symmetry and that the four hydrogen atoms are, therefore, equally shared between the four pyrrole nitrogen atoms.

This result is contrasted with the cation-induced porphyrin dimer.<sup>7a</sup> Due to the position of the 15-crown-5 units (meso position) they were constrained to adopt a lateral complexation of the cation. Consequently, the macrocyclic rings are rotated by ca.  $45^\circ$  (usually) with respect to each other in a staggered dimer.

(36) Gouterman, M.; Holten, D.; Lieberman, E. *Chem. Phys.* **1977**, *25*, 139.

(37) Hochstrasser, R. M. *Molecular Aspects of Symmetry*; W. A. Benjamin Inc.: New York, 1966; p 311. Sharp, J. H.; Lardon, M. *J. Phys. Chem.* **1968**, *72*, 3230.

(38) Lever, A. B. P. *Inorganic Electronic Spectroscopy*, 2nd ed.; Elsevier Science Publishers: Amsterdam, 1984.



This difference in coordination style may explain the difference in cation behavior in the two series. Thus the larger Ba<sup>2+</sup> ion, ineffective in the MtCRPc series, can dimerize the porphyrin whose inter-crown distance can be expanded by further rotation of the porphyrin rings, without weakening the porphyrin-porphyrin  $\pi$ - $\pi$  stabilization. In the MtCRPc case, expanding the crown-crown distance will weaken the Pc-Pc interaction.

It is also interesting that Ca<sup>2+</sup>, which does not dimerize the crown porphyrin and which forms a 1:1 (internal) adduct with 15-crown-5, is, nevertheless, able to generate a cofacial bridged MtCRPc dimer. It is evident that the free energy gained by forming a 1:1 crown ether complex is exceeded, in this case, by forming a 1:2 Ca<sup>2+</sup>:crown species and the cofacial dimeric [MtCRPc]<sub>2</sub>[Ca<sup>2+</sup>]<sub>4</sub>.

Lastly we would like to stress the importance of the eclipsed cofacial dimers realized in the present study. Although several

covalently bound cofacial porphyrin<sup>39</sup> and phthalocyanine<sup>27</sup> dimers have been reported, they are all skewed<sup>39</sup> and/or staggered.<sup>7,27</sup> While not yet proven by X-ray studies, it is likely from the data presented here that these cofacial crown MtCRPc phthalocyanines are perfectly eclipsed and will therefore be archetypes for future studies in this area.

**Acknowledgment.** We thank the Office of Naval Research (Washington) for financial support. We are also indebted to S. Hirao for help in the synthesis of benzo-15-crown-5 dibromide and to H. Lam for NMR assistance.

(39) Collman, J. P.; Chong, A. O.; Jameson, B. G.; Oakley, R. T.; Rose, E.; Schmittou, E. R.; Ibers, J. A. *J. Am. Chem. Soc.* **1981**, *103*, 516. Filler, J. P.; Ravichandran, K. G.; Abdalmuhdi, A.; Tulinsky, A.; Chang, C. K. *Ibid.* **1986**, *108*, 417.

## Pattern of OH Radical Reaction with N<sup>6</sup>,N<sup>6</sup>-Dimethyladenosine. Production of Three Isomeric OH Adducts and Their Dehydration and Ring-Opening Reactions

A. J. S. C. Vieira<sup>1</sup> and S. Steenken\*

Contribution from the Max-Planck-Institut für Strahlenchemie, D-4330 Mülheim, West Germany. Received December 22, 1986

**Abstract:** By use of pulse radiolysis with optical and conductance detection, the reactions in aqueous solution of OH radicals with N<sup>6</sup>,N<sup>6</sup>-dimethyladenosine (DMAdo) were studied. OH reacts with DMAdo with the rate constant  $6.4 \times 10^9 \text{ M}^{-1} \text{ s}^{-1}$  by addition to C-4 (35% probability), to C-5 (19%), and to C-8 (30%) and by H abstraction from the methyl or ribose groups (16%). The resulting OH adducts A-4-OH and A-5-OH on the one hand and A-8-OH on the other undergo unimolecular transformation reactions characterized by different rates (at 20 °C) and activation parameters. With A-4-OH and A-5-OH, the transformations involve OH<sup>-</sup> elimination (dehydration) ( $k = (4.2\text{--}4.9) \times 10^5 \text{ s}^{-1}$ ) to yield the radical cation DMAdo<sup>•+</sup>; with A-8-OH, opening of the imidazole ring occurs ( $k = 9.5 \times 10^4 \text{ s}^{-1}$ ). DMAdo<sup>•+</sup> oxidizes N,N,N',N'-tetramethyl-p-phenylenediamine with  $k = 2.9 \times 10^9 \text{ M}^{-1} \text{ s}^{-1}$ . The OH<sup>-</sup> elimination reactions of A-4-OH and A-5-OH are inhibited by protonation of the radicals, which occurs at pH 4-5 and probably involves N<sup>6</sup> as the proton acceptor. The elimination of OH<sup>-</sup> is prevented also by OH<sup>-</sup>. In contrast, the ring-opening reaction that A-8-OH undergoes is enhanced by OH<sup>-</sup>. A-4-OH, A-5-OH, and A-8-OH and their transformation products differ also with respect to their redox properties. A-4-OH has a low reactivity with O<sub>2</sub>, whereas A-5-OH and A-8-OH are extremely reactive.

It is well established that the interaction of ionizing radiation with living tissue causes severe damage and that the major target is the DNA of the cell nucleus. The most important types of the multiple radiation-induced lesions that occur in DNA are strand breaks, cross-links, and modifications of sugars and of bases. A particularly reactive species, which is to a considerable extent responsible for this damage, is the OH radical, one of the major primary products from the radiolysis of water which, of course, is always present in living cells.

OH radical reactions with the nucleic acid bases<sup>2</sup> and their mononucleosides and nucleotides have been very thoroughly studied over the past 3 decades by a variety of physical and chemical techniques.<sup>3</sup> An important result of these studies is that

the OH radical reacts predominantly by addition to a double bond. In the case of the pyrimidines the C(5)-C(6) bond has been identified as the site of addition, and a mass balance that accounts quantitatively for the fate of the OH radical was obtained by a "redox titration" of the isomeric radicals produced.<sup>4,5</sup> However,

(1) On leave from Instituto Superior Tecnico, Lisbon, Portugal. The work is in partial fulfillment of the Ph.D. requirements.

(2) It has recently been demonstrated that base radicals are able to induce strand breaks: Lemalre, D. G. E.; Bothe, E.; Schulte-Frohlinde, D. *Int. J. Radiat. Biol. Relat. Stud. Phys. Chem. Med.* **1984**, *45*, 351.

(3) For reviews see, e.g.: (a) Scholes, G. In *Radiation Chemistry of Aqueous Systems*; Stein, G., Ed.; Interscience: New York, 1968; p 259. (b) Scholes, G. In *Photochemistry and Photobiology of Nucleic Acids*; Wang, S. Y., Ed.; Academic: New York, 1976; Vol. 1, p 521. (c) Box, H. C. *Radiation Effects, ESR and ENDOR Analysis*; Academic: New York, 1977. (d) Sevilla, M. D. In *Excited States in Organic Chemistry and Biology*; Pullman, B., Goldblum, N., Eds.; Reidel: Dordrecht, 1977; p 15. (e) Hüttermann, J., Köhnlein, W., Teoule, R., Bertinchamps, A. J., Eds. *Effects of Ionizing Radiation on DNA*; Springer: Berlin, 1978. (f) Myers, L. S. In *Free Radicals in Biology*; Pryor, W. A., Ed.; Academic: New York, 1980; Vol. 4, p 95. (g) Bernhard, W. A. *Adv. Radiat. Biol.* **1981**, *9*, 199. (h) Hüttermann, J. *Ultramicroscopy* **1982**, *10*, 25. (i) Greenstock, C. L. *Isr. J. Chem.* **1984**, *24*, 1. (k) Cadet, J.; Berger, M. *Int. J. Radiat. Biol. Relat. Stud. Phys. Chem. Med.* **1985**, *47*, 127. (l) von Sonntag, C.; Schuchmann, H.-P. *Int. J. Radiat. Biol. Relat. Stud. Phys. Chem. Med.* **1986**, *49*, 1.

(4) Fujita, S.; Steenken, S. *J. Am. Chem. Soc.* **1981**, *103*, 2540.

(5) Hazra, D. K.; Steenken, S. *J. Am. Chem. Soc.* **1983**, *105*, 4380.